Improved carrier injection in GaN-based VCSEL via AlGaN/GaN multiple quantum barrier electron blocking layer

D. H. Hsieh,[1] A. J. Tzou,[1,2] T. S. Kao,[1,5] F. I. Lai,[4] D. W. Lin,[1] B. C. Lin,[1] T. C. Lu,[1] W. C. Lai,[3] C. H. Chen,[1] and H. C. Kuo[1,6]

[1]*Department of Photonic & Institute of Electro-Optical Engineering, National Chiao Tung University, Hsinchu 30010, Taiwan*
[2]*Department of Electrophysics, National Chiao Tung University, Hsinchu 30010, Taiwan*
[3]*Department of Photonics, National Cheng Kung University, Tainan 70101, Taiwan*
[4]*Department of Electro-Optics, Yuan-Ze University, Taoyuan 32003, Taiwan*
[5]*tskao@nctu.edu.tw*
[6]*hckuo@faculty.nctu.edu.tw*

Abstract: In this report, the improved lasing performance of the III-nitride based vertical-cavity surface-emitting laser (VCSEL) has been demonstrated by replacing the bulk AlGaN electron blocking layer (EBL) in the conventional VCSEL structure with an AlGaN/GaN multiple quantum barrier (MQB) EBL. The output power can be enhanced up to three times from 0.3 mW to 0.9 mW. In addition, the threshold current density of the fabricated device with the MQB-EBL was reduced from 12 kA/cm^2 (9.5 mA) to 10.6 kA/cm^2 (8.5 mA) compared with the use of the bulk AlGaN EBL. Theoretical calculation results suggest that the improved carrier injection efficiency can be mainly attributed to the partial release of the strain and the effect of quantum interference by using the MQB structure, hence increasing the effective barrier height of the conduction band.

©2015 Optical Society of America

OCIS codes: (140.5960) Semiconductor lasers; (140.7260) Vertical cavity surface emitting lasers.

References and links

1. Y. C. Chi, D. H. Hsieh, C. T. Tsai, H. Y. Chen, H. C. Kuo, and G. R. Lin, "450-nm GaN laser diode enables high-speed visible light communication with 9-Gbps QAM-OFDM," Opt. Express **23**(10), 13051–13059 (2015).
2. A. A. Bergh, "Blue laser diode (LD) and light emitting diode (LED) applications," Phys. Status Solidi A **201**(12), 2740–2754 (2004).
3. S. Izumi, N. Fuutagawa, T. Hamaguchi, M. Murayama, M. Kuramoto, and H. Narui, "Room-temperature continuous-wave operation of GaN-based vertical-cavity surface-emitting lasers fabricated using epitaxial lateral overgrowth," Appl. Phys. Express **8**(6), 062702 (2015).
4. Y. Higuchi, K. Omae, H. Matsumura, and T. Mukai, "Room-temperature CW lasing of a GaN-based vertical-cavity surface-emitting laser by current injection," Appl. Phys. Express **1**, 121102 (2008).
5. G. S. Huang, T. C. Lu, H. H. Yao, H. C. Kuo, S. C. Wang, C. W. Lin, and L. Chang, "Crack-free GaN/AlN distributed bragg reflectors incorporated with GaN/AlN superlattices grown by metalorganic chemical vapor deposition," Appl. Phys. Lett. **88**(6), 061904 (2006).
6. T. C. Lu, S. W. Chen, T. T. Wu, P. M. Tu, C. K. Chen, C. H. Chen, Z. Y. Li, H. C. Kuo, and S. C. Wang, "Continuous wave operation of current injected GaN vertical cavity surface emitting lasers at room temperature," Appl. Phys. Lett. **97**(7), 071114 (2010).
7. G. Cosendey, A. Castiglia, G. Rossbach, J. F. Carlin, and N. Grandjean, "Blue monolithic AlInN-based vertical cavity surface emitting laser diode on free-standing GaN substrate," Appl. Phys. Lett. **101**(15), 151113 (2012).
8. S. Nakamura, "The roles of structural imperfections in InGaN-based blue light-emitting diodes and laser diodes," Science **281**(5379), 956–961 (1998).
9. S. Nakamura, M. Senoh, S. Nagahama, N. Iwasa, T. Yamada, T. Matsushita, Y. Sugimoto, and H. Kiyoku, "Room-temperature continuous-wave operation of InGaN multi-quantum-well-structure laser diodes with a long lifetime," Appl. Phys. Lett. **70**(7), 868–870 (1997).
10. C. T. Yu, W. C. Lai, C. H. Yen, and S. J. Chang, "Effects of InGaN layer thickness of AlGaN/InGaN superlattice electron blocking layer on the overall efficiency and efficiency droops of GaN-based light emitting diodes," Opt. Express **22**(S3 Suppl 3), A663–A670 (2014).

#245913 Received 15 Jul 2015; revised 8 Sep 2015; accepted 9 Sep 2015; published 7 Oct 2015

11. M. H. Kim, M. F. Schubert, Q. Dai, J. K. Kim, E. F. Schubert, J. Piprek, and Y. Park, "Origin of efficiency droop in GaN-based light-emitting diodes," Appl. Phys. Lett. **91**(18), 183507 (2007).
12. C. H. Wang, C. C. Ke, C. Y. Lee, S. P. Chang, W. T. Chang, J. C. Li, Z. Y. Li, H. C. Yang, H. C. Kuo, T. C. Lu, and S. C. Wang, "Hole injection and efficiency droop improvement in InGaN/GaN light-emitting diodes by band-engineered electron blocking layer," Appl. Phys. Lett. **97**(26), 261103 (2010).
13. J. A. Lott and K. J. Malloy, "Orange vertical cavity surface emitting lasers," in *CLEO/Pacific Rim '95, Pacific Rim Conference on Lasers and Electro-Optics* (OSA, 1995), pp. 258–259.
14. R. B. Chung, C. Han, C. C. Pan, N. Pfaff, J. S. Speck, S. P. DenBaars, and S. Nakamura, "The reduction of efficiency droop by $Al_{0.82}In_{0.18}N$/GaN superlattice electron blocking layer in (0001) oriented GaN-based light emitting diodes," Appl. Phys. Lett. **101**(13), 131113 (2012).
15. Y. Y. Zhang and Y. A. Yin, "Performance enhancement of blue light-emitting diodes with a special designed AlGaN/GaN superlattice electron-blocking layer," Appl. Phys. Lett. **99**(22), 221103 (2011).
16. Y. Y. Lin, R. W. Chuang, S. J. Chang, S. Li, Z. Y. Jiao, T. K. Ko, S. J. Hon, and C. H. Liu, "GaN-based LEDs with a chirped multiquantum barrier structure," IEEE Photonics Technol. Lett. **24**(18), 1600–1602 (2012).
17. S. J. Chang, Y. Y. Lin, C. H. Liu, S. Li, T. K. Ko, and S. J. Hon, "Numerical simulation of GaN-based LEDs with chirped multiquantum barrier structure," IEEE J. Quantum Electron. **49**(4), 436–442 (2013).
18. T. Takagi, F. Koyama, and K. Iga, "Design of multiquantum barrier (MQB) and experimental verification of electron wave reflection by MQB," Electron. Commun. Jpn. **75**, 527–535 (1992).
19. K. Iga, H. Uenohara, and F. Koyama, "Electron reflectance of multiquantum barrier (MQB)," IEEE Electron. Lett. **22**(19), 1008–1010 (1986).
20. C. S. Xia, Z. M. S. Li, Z. Q. Li, and Y. Sheng, "Effect of multiquantum barriers in performance enhancement of GaN-based light-emitting diodes," Appl. Phys. Lett. **102**(1), 013507 (2013).
21. W. J. Liu, X. L. Hu, L. Y. Ying, S. Q. Chen, J. Y. Zhang, H. Akiyama, Z. P. Cai, and B. P. Zhang, "On the importance of cavity-length and heat dissipation in GaN-based vertical-cavity surface-emitting lasers," Sci. Rep. **5**, 9600 (2015).
22. C. Holder, J. S. Speck, S. P. DenBaars, S. Nakamura, and D. Feezell, "Demonstration of nonpolar GaN-based vertical-cavity surface-emitting lasers," Appl. Phys. Express **5**(9), 092104 (2012).
23. PICS3D (Photonic Integrated Circuit Simulator in 3D) by Crosslight Software, Inc., Burnaby, Canada, (2005).

1. Introduction

Over the past years, GaN-based vertical-cavity surface-emitting lasers (VCSELs) attracted significant attentions due to their superior characteristics over the GaN-based edge-emitting lasers (EELs), such as the circular beam shape, on-wafer testing, low threshold current, and single longitudinal mode operation. Furthermore, GaN-based VCSELs exhibit potential applications in the laser displays, optical-storage systems and visible-laser-communications [1,2]. However, compared to the GaN-based EELs, which had been commercialized for decades. GaN-based VCSELs still have many problems, which mainly arise from the obstacle of growing high quality GaN/Al(Ga)N distributed Bragg reflector (DBR) owing to the large lattice mismatch between GaN and Al(Ga)N. To overcome this problem, numbers of groups spent numerous effort on the hybrid structure, which uses dielectric DBR mirror to replace the GaN/Al(Ga)N DBR [3,4]. However, fabrication of hybrid structures require complicate process including laser lift-off, chemical-mechanical polishing (CMP), such additional process increase the risk of deterioration of the device quality. In our previous research [5], we have successfully produced an epitaxial DBR with high reflectivity by inserting the GaN/AlN super-lattice structure into the GaN/AlN DBR pairs. By using this method, the first GaN-based VCSEL operated at room temperature and under the CW injection was achieved with the GaN/AlN bottom DBR and dielectric top DBR [6]. Although the use of super-lattice strain-released structure can improve the quality of DBR layers, it would also increase the difficulty and time cost of epitaxy. Recently, GaN-based devices grown on the GaN substrate had been reported that, the defect density can be reduced effectively, and hence the better devices performance can be expected [7].

Despite the growth of high quality device, further serious issues in GaN-based materials can be related to: 1) the strong spontaneous and piezoelectric polarization fields in c-plane wurtzite GaN-based materials [8,9] and hence the quantum-confined Stark-effect (QCSE). 2) Large difference between electron and hole mass can lead to that, crucial electron overflow outside the tilted active region which suffers significant QCSE, and hence the large leakage current. To solve this issue, the insertion of AlGaN electron-blocking-layer (EBL) between MQW and p-GaN spacer is a useful strategy to suppress electron overflow [10,11], but the high Al content also causes a serious band bending between the last barrier of MQW and EBL

#245913 Received 15 Jul 2015; revised 8 Sep 2015; accepted 9 Sep 2015; published 7 Oct 2015
© 2015 OSA

layer, which will lower the electron blocking ability. Diverse kinds of EBL had been proposed in GaN-based light emitting diodes (LED) to improve the ability of suppressing leakage current, such as Al-graded bulk AlGaN EBL, ternary InAlN EBL, AlGaN/GaN uniform multiple quantum barrier (UMQB) EBL [10,12–15] and AlGaN/GaN chirped-MQB (CMQB) EBL [16,17], the use of MQB EBL was also proposed in InP-based VCSELs, which shows a superior ability in reducing the carrier leakage from active region [13]. Among these different design of EBL structures for LEDs, UMQB EBL structures can be regarded as a promising method, which is because of its strain release ability [10], and high virtual potential height due to the quantum interference effect [18–20]. With the use of CMQB EBL, it could provide even higher electron blocking ability with gradual increase/decrease in MQB pair thickness [16,17]. However, to the best of our knowledge, in GaN-based VCSELs, the EBL structures remain similar to the conventional bulk AlGaN EBL in GaN-based LEDs [3,7,21,22]. In this report, the GaN-based VCSEL structures are grown on the GaN substrate, and the AlGaN/GaN MQB EBL is adopted to improve the VCSEL device performance. Compared to the VCSEL using conventional AlGaN bulk EBL, the using of MQB EBL can effectively reduce the threshold current density from 12 kA/cm^2 (9.5 mA) to 10.6 kA/cm^2 (8.5 mA), and increase the optical power from 0.3 mW to 0.9 mW.

2. Experiments

Figure 1 shows the schematic illustration of the GaN-based VCSEL structure with bulk EBL (C-VCSEL) and MQB EBL (MQB-VCSEL). The epitaxial layer was grown on a GaN substrate (Sumitomo corp.) by the metal-organic chemical vapor deposition (MOCVD) method. The conventional GaN-based VCSEL structure (C-VCSEL) consists a 30 nm GaN nucleation layer, followed by a 25 pairs un-doped AlN/GaN DBR at bottom as a reflector. In this structure, the optical cavity is formed by an 880 nm Si-doped n-type GaN (n-doping = 5 × 10^{18} cm^{-3}), five pairs of $In_{0.15}GaN$ (4 nm)/$In_{0.02}GaN$ (8 nm) MQWs, a 20 nm Mg-doped p-type $Al_{0.2}Ga_{0.8}N$ (p-doping = 3 × 10^{17} cm^{-3}) electron blocking layer (EBL), and a 100 nm Mg-doped p-type GaN (p-doping = 5 × 10^{17} cm^{-3}). After the growth of optical cavity, a 200 nm SiN_x layer is deposited onto p-GaN layer by plasma-enhanced chemical vapor deposition (PECVD), and a circular aperture of 5 μm in radius, is formed to confine the current. In order to acquire better current spreading, an indium-tin-oxide (ITO) layer is deposited sequentially on the whole mesa region, and then annealed by the rapid thermal annealing process at 600 °C for 10 min. The top reflector, which consists 10 pairs Ta_2O_5/SiO_2 dielectric DBR, is then deposited onto the ITO layer. In order to have a comparison to the conventional VCSEL device, we design a new type of the GaN-VCSEL with MQB EBL (MQB-VCSEL), where the 20 nm $Al_{0.2}GaN$ bulk EBL is replaced by five pairs Mg-doped $Al_{0.15}Ga_{0.8}N$ (2 nm)/GaN (2 nm) super-lattice layer and the p-doping is equal to 3 × 10^{17} cm^{-3}.

The electrical and optical characteristics of these two type of VCSEL devices are first investigated by conducting simulations with the Photonic Integrated Circuit Simulator in 3D (PICS3D) software (Crosslight corp) [23]. The PICS3D is an advanced simulator based on finite element analysis, which were employed to solve the Poisson's equation, current continuity equations, carrier transport equations, complex wave equations, and rate equations of VCSEL devices in the cylindrical coordinates. The spontaneous and piezoelectric polarization in GaN-based materials are also considered in the simulator to calculate the built-in polarization field. Both the longitudinal and transverse optical modes are solved by the effective index (EIM) model. The use of EIM model is beneficial to the device with complex structural variation in lateral direction. Furthermore, to investigate the quantum tunneling effect within different EBL structures, additional quantum interference effect is also considered during the calculation.

#245913 Received 15 Jul 2015; revised 8 Sep 2015; accepted 9 Sep 2015; published 7 Oct 2015
© 2015 OSA

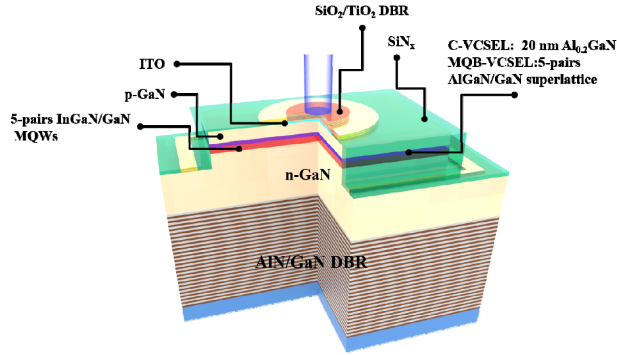

Fig. 1. Schematic structure of GaN-based VCSEL with AlGaN bulk EBL (C-VCSEL) and AlGaN/GaN MQB EBL (MQB-VCSEL).

3. Results and discussion

First, Figs. 2(a) and 2(b) show the simulated band diagrams of C-VCSEL and MQB-VCSEL by the PICS3D simulator, respectively. Both band-diagrams are taken at 12 kA/cm^2. From the simulation results of C-VCSEL, one can see that the band bending occurs at active regions. Such a band bending phenomenon is resulted from the severe polarization-induced electric field, which may lower the wave-function overlap of electrons and holes, thus giving less spontaneous emission coupled into the lasing mode. Furthermore, a downward band bending occurs at the interface between the last quantum barrier (GaN) and EBL ($Al_{0.2}GaN$) due to the large lattice mismatch between the last GaN quantum barrier in active region and $Al_{0.2}GaN$, which resulted in an electron barrier height of 331 meV. Compared with the C-VCSEL structure as a counterpart, as shown in Fig. 2(b), because of the strain at the interface between quantum barrier and EBL is released by the use of super-lattice structure [10]. The electron barrier height in MQB-VCSEL has been effectively increased to 431 meV, and thus a better electron blocking ability can be expected. Addition to the increased electron barrier height, MQB-VCSEL also show a smaller hole barrier height (310 meV) than the one in C-VCSEL (332 meV). The reduced hole barrier height can be beneficial to the hole transport in MQB-VCSEL.

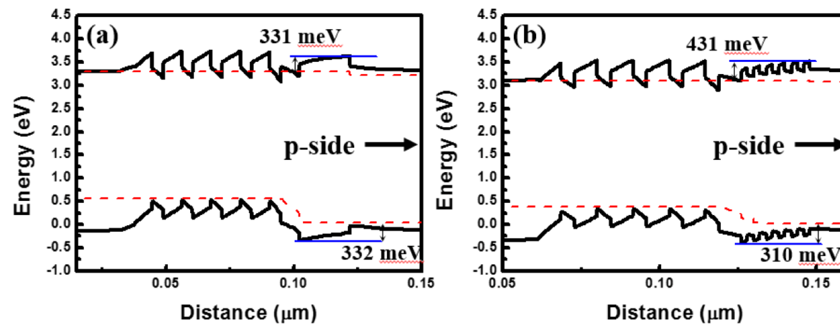

Fig. 2. Band diagram of the GaN-based VCSEL structures with (a) conventional bulk $Al_{0.2}GaN$ EBL (C-VCSEL) and (b) super-lattice $Al_{0.15}GaN$/GaN EBL (MQB-VCSEL) taken at bias current density of 12 kA/cm^2. The simulated barrier height for electrons/holes is 331/332 meV for C-VCSEL, and 431/310 meV for MQB-VCSEL, respectively.

Besides the higher potential barriers for electrons obtained in the MQB-VCSEL structure, Figs. 3(a) and 3(b) present the calculated electron and hole reflectance probability versus carrier energy for bulk and MQB EBL. In Fig. 3(a), it shows a higher probability for electrons being reflected by the MQB EBL in higher energy region than that of bulk EBL structure. Such a result caused by the quantum interference effect within MQB structure [18,19] leads to

#245913 Received 15 Jul 2015; revised 8 Sep 2015; accepted 9 Sep 2015; published 7 Oct 2015
© 2015 OSA

the higher effective potential height. For both EBL structures, the electron and hole reflectance probability exhibit significant oscillation in higher energy region, which is similar to the Ramsauer-Townsend effect and the carrier/atom scattering [20]. However, the low-energy dip appears in the electron and hole reflectance probability of MQB EBL is affected by the electron tunneling effect through MQB layer. Regarding the reflectance of holes, although MQB structure shows a narrower high reflectance region (0 to 120 meV), it shows a relative high reflectance at higher energy region (224 to 300 meV) due to the hole/atom scattering.

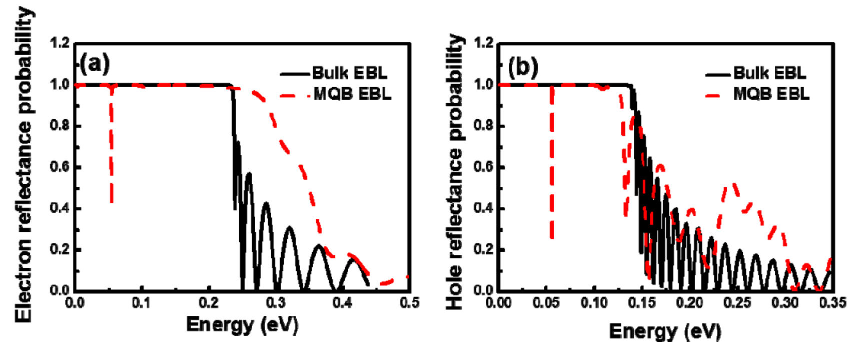

Fig. 3. The (a) electron and (b) hole reflectance probability versus carrier energy of different EBL structures in C-VCSEL and MQB-VCSEL. The dips both in electron and hole reflectance probability spectra of the MQB-VCSEL are due to the tunneling effect in constituent super-lattice structure.

The two-dimensional mappings of electron, hole and total current density are respectively shown in the upper row in Figs. 4(a)-4(c) for C-VCSEL and bottom row in Figs. 4(d)-4(f) for MQB-VCSEL structures. Comparing the electron current density distributions shown in Fig. 4(a) and 4(d), we can see that most electrons pass through the MQW region to the p-GaN layer along the aperture edge in C-VCSEL, resulting in a large leakage current. In the MQB-VCSEL structure, due to the better electron blocking ability, the electron density in MQW region for MQB-VCSEL is obviously larger than that for C-VCSEL, hence the leakage current can be efficiently suppressed. From the hole current density mappings in Fig. 4(b) and 4(e), no obvious discrepancy occurs between the C-VCSEL and MQB-VCSEL, attributing to the comparable hole barrier at valance band in these two structures, and the compensation of hole reflectance by higher energy hole/atom scattering effect. However, because of the relative larger mobility of electrons than holes in nitride-based materials, the confinement of electrons is more efficient than the holes injection. As a consequence, from the total current densities as shown in Figs. 4(c) and 4(f), it can be seen that there are more total current and less leakage current in the MQB-VCSEL than that in the C-VCSEL.

#245913 Received 15 Jul 2015; revised 8 Sep 2015; accepted 9 Sep 2015; published 7 Oct 2015
© 2015 OSA

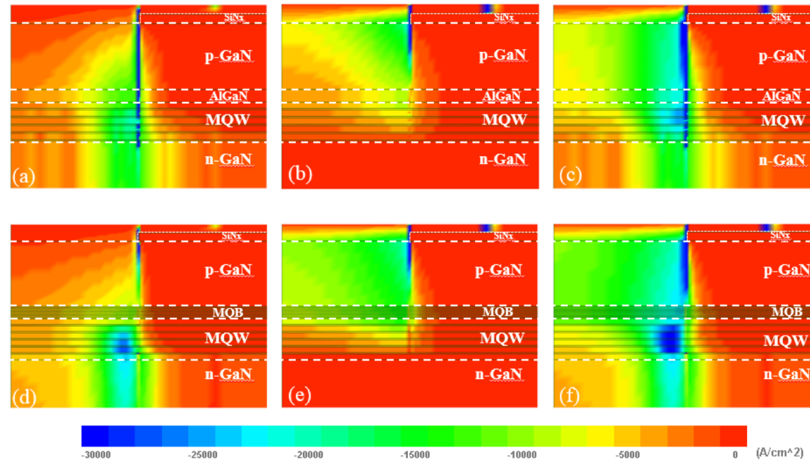

Fig. 4. Two dimensional mappings of electron, hole, and total current density flow in (a)─(c) for the C- VCSEL and (d)─(f) for MQB-VCSEL.

Figure 5 shows the experimental and simulation results of the output power-current density curves in the VCSEL devices. The performance of VCSEL devices were measured at room temperature under a CW current operation, for which the threshold current densities are about 12 kA/cm^2 (9.5 mA) and 10.6 kA/cm^2 (8.5 mA) for C-VCSEL and MQB-VCSEL, respectively. The experimental current-voltage character shown in the inset of Fig. 5 indicates that, the turn-on voltage is reduced from 4.7 V in C-VCSEL to 4.5 V in MQB-VCSEL at 2 kA/cm^2. The resistance shows a 5% reduction by using the MQB EBL, which could be due to the lower barrier height for holes. The simulated power-current density results for both cases show a good agreement with experimental results. As mentioned above, this result is caused by the better electrons blocking ability for MQB-VCSEL due to the strain release and the higher virtual potential barrier provided by super-lattice structure. Furthermore, because of the increased injection efficiency, the output power of MQB-VCSEL shows a maximum power of 0.9 mW at 23 kA/cm2, which is about three times higher than the optical power of 0.3 mW at 19 kA/cm^2 for C-VCSEL.

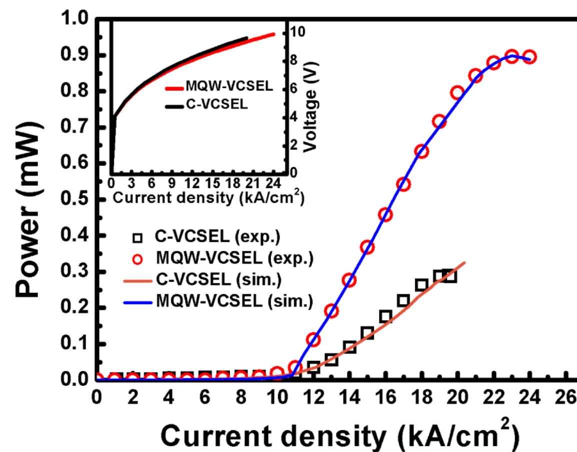

Fig. 5. Comparison of the experimental and simulation results of the power-current density curve in C-VCSEL and MQB-VCSEL structures, and with the experimental current density-voltage characteristic shown in the inset.

#245913 Received 15 Jul 2015; revised 8 Sep 2015; accepted 9 Sep 2015; published 7 Oct 2015
© 2015 OSA

4. Conclusions

In conclusion, VCSELs with conventional bulk AlGaN EBL and AlGaN/GaN multiple-quantum-barrier EBL have been demonstrated and compared. The electrical and optical properties are both observed in experimental measurement and theoretical calculation. The results show a reduction in threshold current density from 12 kA/cm^2 (9.5 mA) to 10.6 kA/cm^2 (8.5 mA), and a three times improvement of optical output power by using AlGaN/GaN multiple-quantum-barrier EBL from 0.3 mW to 0.9 mW. The reason for this improved performance of the VCSEL with MQB EBL was observed via theoretical calculation, which suggests the higher injection efficiency in the active region due to the better electron blocking ability. The enhanced electron blocking ability can be attributed to the released strain by using MQB structure, and the higher virtual potential barrier experienced by electrons due to the quantum interference effect.

Acknowledgments

The authors would like to thank Professor Bao-Ping Zhang of Xiamen University, China for their technical support. This work was funded by the Ministry of Science and Technology of Taiwan under Grant No. MOST 104-3113-E-009 –002 -CC2

#245913 Received 15 Jul 2015; revised 8 Sep 2015; accepted 9 Sep 2015; published 7 Oct 2015
© 2015 OSA